University of Groningen

Proton-proton bremsstrahlung towards the elastic limit at 190 MeV incident beam energy

Mahjour-Shafiei, M; Amir Ahmadi, HR; Bacelar, JCS; Castelijns, R; Ermisch, K; van Garderen, ED; Gasparic, I.; Harakeh, MN; Kalantar-Nayestanaki, N; Kis, M

IMPORTANT NOTE: You are advised to consult the publisher's version (publisher's PDF) if you wish to cite from it. Please check the document version below.

Document Version
Publisher's PDF, also known as Version of record

Link to publication in University of Groningen/UMCG research database

Proton–proton bremsstrahlung towards the elastic limit at 190 MeV incident beam energy

M. Mahjour-Shafiei [a,b,*], H.R. Amir-Ahmadi [a], J.C.S. Bacelar [a], R. Castelijns [a], K. Ermisch [a],
E.D. van Garderen [a], I. Gašparić [c], M.N. Harakeh [a], N. Kalantar-Nayestanaki [a], M. Kiš [a,1],
H. Löhner [a], O. Scholten [a]

[a] *Kernfysisch Versneller Instituut, Zernikelaan 25, 9747 AA Groningen, The Netherlands*
[b] *Physics Department, Tehran University, P.O. Box 14395/547, Tehran, Iran*
[c] *Rudjer Bošković Institute, Zagreb, Croatia*

Abstract

A series of nucleon–nucleon bremsstrahlung ($NN\gamma$) experiments at 190 MeV incident beam energy have been performed at KVI in order to gain more insight into the dynamics governing the bremsstrahlung reaction. After initial measurements wherein the bremsstrahlung process was studied far away from the elastic limit, a new study was used to probe the process nearer to the elastic limit by measuring at lower photon energies. Measured cross sections and analyzing powers are compared with the predictions of a microscopic model and those of two soft-photon models. The theoretical calculations overestimate the data by up to $\approx 30\%$, for some kinematics.

The nucleon–nucleon (NN) interaction is the corner-stone of any model dealing with nuclear systems. It is, therefore, vital to have a good understanding of the NN potential before searching for smaller effects such as the three nucleon force. The NN potential can be addressed by studying the deuteron as the simplest bound state, or by investigating observables of NN scattering. As the result of NN-elastic scattering experiments performed in the last decades, a very extensive data set has emerged. On the theoretical side, modern potentials [1–3] have been constructed which fit the data with a χ^2 close to unity. Since the predictions of different realistic potential models are nearly the same for elastic NN scattering, they are said

to be "data-equivalent". It has been a long-standing hope to distinguish among these models by using the observables of proton–proton bremsstrahlung (hereafter $pp\gamma$) [4–6], which involves a photon in addition to two nucleons in the final state. However, due to the fact that the predictions of bremsstrahlung models using various potentials are very similar [7], and the differences between them are smaller than their differences with the data, the experimental $pp\gamma$ data can be used to understand the underlying physics of the nucleon–nucleon bremsstrahlung process.

In 1996, a series of measurements were performed at KVI to study $pp\gamma$ at 190 MeV incident beam energy. The first data at small proton opening angles, corresponding to large photon energies, typically 65 MeV, were published subsequently [8–11]. In continuation of that work and in order to cover a much larger area of the available phase space, a new experiment using a new setup was performed. This setup was designed in a way

---

* Corresponding author.
  E-mail address: shafiei@kvi.nl (M. Mahjour-Shafiei).
[1] Present address: Rudjer Bošković Institute, Zagreb, Croatia.

to be able to measure larger proton opening angles or equivalently smaller photon energies, typically 45 MeV, thus moving towards the elastic limit. At the elastic limit all gauge-invariant microscopic models should yield predictions that converge to the results of the calculations based on the soft-photon theorem as these calculations are by construction in agreement with the results of elastic scattering. In this Letter, the results of this experiment, closer to the elastic limit, are compared to microscopic [12–15] and soft-photon model (SPM) calculations [16,17].

In the present experiment, a proton beam with average intensity and polarization of 1.5 nA and 0.6, respectively, was delivered by the AGOR cyclotron. The beam was impinged on a liquid hydrogen target with a nominal thickness of 6 mm [18]. SALAD (small-angle large-acceptance detector) [19] was employed to detect protons at forward angles, and to measure their energies and coordinates. It consists of a MWPC placed 30 cm away from the target (as opposed to 50 cm in the previous measurements [8–11]) and two arrays of plastic scintillators. The MWPC is capable of determining the angular coordinates of protons with a resolution of $0.7°$. The first array of scintillators, called energy scintillators, consists of 24 scintillator elements. These scintillators are made thick enough to stop all protons originating from the bremsstrahlung reaction, thereby measuring their energies. However, most of the elastically-scattered protons punch through the energy layer and reach the second array of scintillators, the Veto scintillators. The Veto scintillators, consisting of 26 scintillators, are deployed to identify elastically-scattered protons. This identification is used to reject events, which are not $pp\gamma$ events, at the first trigger level. In the chosen geometry, SALAD is capable of detecting protons with polar angles between $10°$ and $36°$ with a high efficiency. However, the azimuthal-angle coverage of the detector is not 100% for polar angles larger than $28°$ and goes to zero at polar angle of $\sim 40°$. The backward hemisphere of plastic ball [20], consisting of 340 phoswich detector modules, was used to detect photons scattered to angles larger than $90°$. The opening angle of each module is $10°$, providing a good enough resolution in the determination of the coordinates of the photons for the kinematical reconstruction. The photon detector covered a polar angular range of $90°$ to $160°$ with a full azimuthal coverage. With this setup all the outgoing particles of the bremsstrahlung process were detected.

In the data analysis, both elastic and inelastic (bremsstrahlung) channels were analyzed. Asymmetries were also obtained from the data. By fitting the asymmetries for elastic scattering to the predictions of a global data analysis such as PWA93 [21], the beam polarization is determined with high accuracy. In this way, the systematic uncertainty in the beam polarization was kept below 0.005. The elastic-scattering data were also used as a monitor of the system.

The main trigger, called $pp\gamma$ trigger, is made when within a time window of 100 ns, the number of hits detected by energy scintillators minus that detected by the Vetos is equal or larger than two, along with at least one hit on the plastic ball. Using this trigger the background originating from the elastically-scattered protons was considerably suppressed. Yet, only 1.5%

of the events read-out through this trigger are real $pp\gamma$ events; the rest are background events originating primarily from elastic scattering. As the first step in $pp\gamma$ event selection, a gate is set on the TDC spectra of SALAD scintillators, selecting the prompt coincidences. This way the protons with the right arrival-time difference are selected. On the plastic-ball side, the charged particles are identified by pulse-shape analysis and eliminated.

The kinematics of proton–proton bremsstrahlung involves three particles, resulting in nine kinematic variables, polar and azimuthal angles of the protons and the photon which are denoted as, θ_1, θ_2, θ_γ, ϕ_1, ϕ_2, and ϕ_γ respectively. However, it is more conventional to use two other variables, namely non-coplanarity angle (ϕ_{nonco}) and the azimuthal angle of the event (ϕ_{event}), instead of ϕ_1 and ϕ_2. ϕ_{nonco} is the angle between the projected momentum of each proton onto the x–y plane and a plane containing the incoming beam but rotated so much to make the same angle with both protons. This plane is called the coplanar plane. ϕ_{event} is the angle between a vector normal to the coplanar plane and y-axis. The normal vector is on the same side of the coplanar plane as the protons are. Due to energy and momentum conservation, only five of these variables are needed to kinematically reconstruct an event. In this experiment, all nine variables were measured, providing four over-determined variables. The angular coordinates of the protons and the polar angle of the photon were used as input for the event reconstruction as they were measured with relatively better resolution than other variables. The reconstruction leads to two physically acceptable solutions. There is a unique way to label and distinguish the solutions. Labeling the solutions give rise to the labeling of the protons (see Ref. [11] for more details). When moving towards the elastic limit, one can see that the non-coplanarity angle approaches zero. For this limit, the definition of proton 1 and proton 2 is rather trivial. The proton which is on the same side as the photon with respect to the beam direction is proton 1 and the other one is proton 2. Subsequently, by plotting the difference between the reconstructed and measured energies of proton 1 versus the same quantity for proton 2 a pattern emerges, highlighting the most probable proton–proton bremsstrahlung events as shown in Fig. 1. These events are selected by applying the graphical cut indicated in the figure. Further background rejection is done by requiring the measured energy of the photon to be above 25 MeV, as a study of the background revealed that the background on the plastic-ball side mainly stems from low-energy photons. The effect of this cut was corrected for by Monte Carlo simulations. The last over-determined variable, the azimuthal angle of the photon was used to estimate the remaining background. After applying all cuts, the remaining background is estimated to be generally less than 0.5%.

In this experiment there were four types of inefficiencies, namely, data-acquisition dead-time, MWPC inefficiency, trigger inefficiency, and photon detection inefficiency. The dead-time and the MWPC inefficiency were typically 50% and 5%, respectively. Trigger inefficiency is the fraction of the $pp\gamma$ events which are lost at the level of defining the main event trigger, and was estimated to be around 4%. Finally, the photon
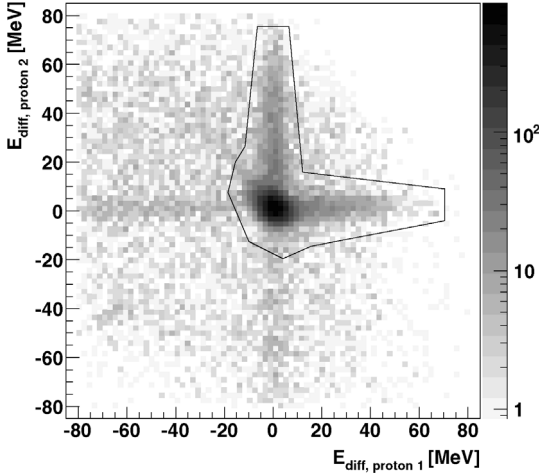
Fig. 1. The difference between the reconstructed and measured energies of proton 1 versus that of proton 2, along with the graphical cut used in the analysis. The two arms stretched to the right and above the kinematical locus originate from good events in which a proton has undergone a hadronic interaction. The much less-populated arms to the left and below the kinematical locus come from events in which a pile-up of particles existed. The gray-scale indicating the intensity is logarithmic.

Fig. 2. Cross sections, analyzing powers, and relative energies, for the combination $\theta_1 = 19°$, $\theta_\gamma = 135°$ ($\theta_2 = 19°$, $\theta_\gamma = 135°$) in the left (right) panel as a function of θ_2 (θ_1). Only statistical errors are shown here. An absolute systematic error (point-to-point error) of 6% (3%) is not shown for the cross section. The systematic error of 2% in the analyzing powers is negligible compared to the statistical errors. The solid, dotted and dash-dotted lines in the top and middle panels are the predictions of the microscopic model [12–15], tu-SPM and ak-SPM [16,17,22,23], respectively.

detection inefficiency is the probability that a photon escapes detection, or is thrown away by the 25 MeV cut on the energy spectrum of the photon in the analysis. This inefficiency was obtained using GEANT simulations. As the simulations revealed, the photon detection inefficiency decreases from 80% to 50% as a function of the energy of the incident photon which is dependent on the kinematics of the event. All these inefficiencies, which are generally low with the exception of photon detection efficiency, have been applied in a proper manner for each data point presented later. For the absolute cross sections, the high-precision data obtained in an earlier KVI experiment [8–11] were used for normalization purposes, as there was a reasonable overlap in the kinematics of the two experiments. In the region of overlapping kinematics with the previous experiment, there is a very good agreement in the angular-distribution measurements.

For the data presented here, the ϕ_{nonco} is kept below 5° and an integration over ϕ_{event} has been performed for the cross sections. In the left (right) panel of Fig. 2, the cross sections and analyzing powers are shown for the kinematic combination $\theta_1 = 19°$, $\theta_\gamma = 135°$ ($\theta_2 = 19°$, $\theta_\gamma = 135°$) as a function θ_2 (θ_1). The cross sections are depicted in the top panels, while the analyzing powers are presented in the middle ones for the same kinematics. In the figure, only statistical errors are shown. The overall systematic error on the normalization of the cross-section data, is 6%. The point-to-point systematic error is around 3%. The data are compared with the prediction of the microscopic model of Martinus et al. [12] and Cozma et al. [14,15], solid curve, and that of tu-SPM [16,17] and another soft-photon model (here called ak) [16,22,23], dotted and dash-dotted curves, respectively. The results of the two soft-photon models shown here have been obtained using various approximations for the bremsstrahlung amplitude all obeying the soft-photon theorem [22,23]. In the covariant microscopic
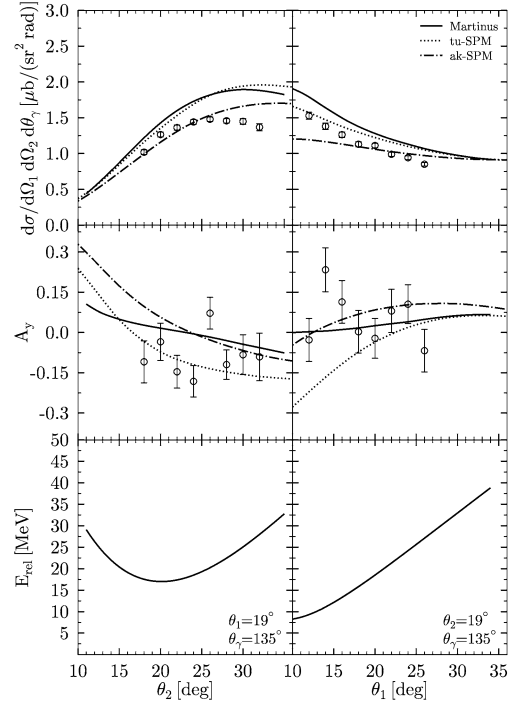
model, in addition to the single- and double-scattering contributions, meson-exchange currents and Δ-isobar contributions have also been included. Gauge invariance is not obeyed in the microscopic model, while soft-photon models are gauge invariant by construction. In the bottom panels a kinematical variable, namely the relative energy of the protons, is depicted. This variable, denoted as E_{rel}, is the invariant mass of protons in the exit channel minus their rest masses, $E_{\text{rel}} = \sqrt{(E_1 + E_2)^2 - (\vec{p}_1 + \vec{p}_2)^2} - 2m_p$, where E_1 ($\vec{p}_1$) and E_2 ($\vec{p}_2$) are the energies (momenta) of protons 1 and 2, respectively ($\hbar = c = 1$). E_{rel} is a measure of how far the kinematics is from the elastic channel. Also, one expects large final-state interactions for small E_{rel}. The photon energy in the C.M. frame can be expressed as $E_\gamma^{\text{C.M.}} \approx E_{\text{in}}^{\text{C.M.}} - E_{\text{rel}} \approx 93 - E_{\text{rel}}$ for the present experiment, where $E_{\text{in}}^{\text{C.M.}}$ represents the available kinetic energy for the entrance channel in the center of mass. The larger the relative energy, the smaller the photon energy and, therefore, the closer the kinematics to the elastic limit (at the elastic limit, $E_{\text{rel}} \approx 93$ MeV).

In Fig. 3, the cross sections, analyzing powers, and relative energies are shown as a function of θ_γ, the polar angle of the photon, for an asymmetric combination ($\theta_1 = 33°$, $\theta_2 = 24°$) along with its kinematical mirror. Also here, the errors shown in the figure indicate statistical errors only. Again, one has to consider 6% (3%) absolute (point-to-point) systematic error for the cross section.
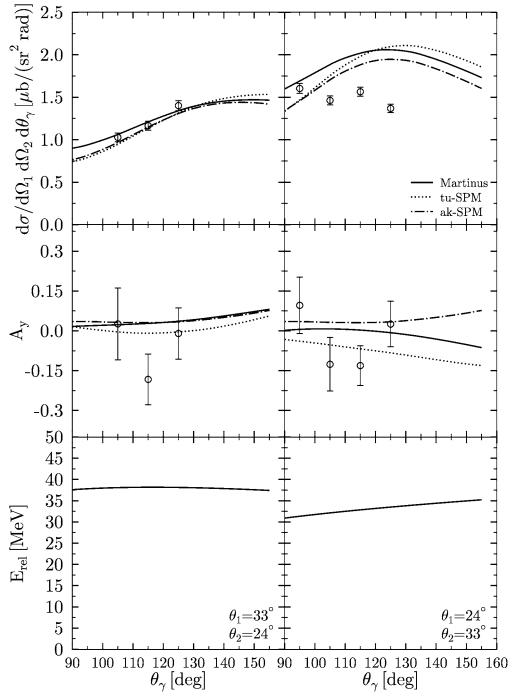
Fig. 3. Cross sections, analyzing powers, and relative energies for the combination $\theta_1 = 33°$, $\theta_2 = 24°$ ($\theta_1 = 24°$, $\theta_2 = 33°$) in the left (right) panel as a function of θ_γ. For explanation of curves and errors, see the caption of Fig. 2.

Fig. 4. Same as Fig. 2 except for $\theta_1 = 25°$, $\theta_\gamma = 95°$ ($\theta_2 = 25°$, $\theta_\gamma = 95°$) in the left (right) panels.

The main feature in Fig. 3 is the better agreement between the cross-section data and the prediction of the theoretical models where $\theta_1 > \theta_2$. The same observation can be made from the plot on the top-left panel of Fig. 2, where the agreement between the data and the theoretical calculations gradually worsens as θ_2 increases. This is not understood presently. Furthermore, there seems to be no clear trend for the level of agreement between the data and the theoretical prediction on the relative energy for the kinematics shown here. This is contrary to our earlier observation for higher photon energies [11] where the disagreement went from 40% to 20% when one moved from $E_{rel} = 5$ MeV to $E_{rel} = 25$ MeV. In contrast to most of the kinematics covered in this measurement, the data point with $\theta_\gamma = 95°$, top-right in Fig. 3, comes very close to the theoretical curves. This observation was made for all kinematics with $\theta_\gamma = 95°$; see Fig. 4.

The statistical errors of the analyzing powers are too large to draw any conclusions. However, theory and experiment are in qualitative agreement since both give small values for this observable. One should note that the error bars for the analyzing powers presented here are relatively larger than those for the cross sections due to the fact that the beam used in this measurement was not fully polarized and the scale chosen for the figures enhances these small numbers.

If one compares the differences between theoretical and experimental cross sections for the kinematics of the present work with those of Refs. [8–11] (called "the previous"), the following conclusions can be made: (i) Even for the present experiment where the photon energy is considerably lower than in the previous one, the differences between the two SPMs is still rather large. Higher-order terms beyond those of the soft-photon the-
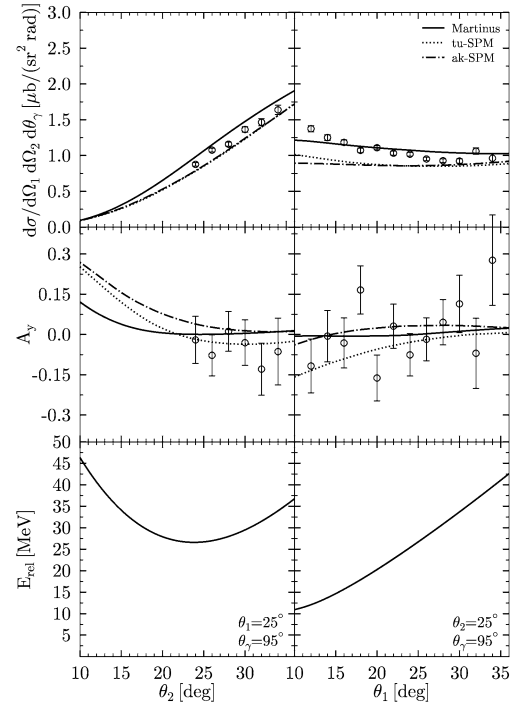
orem are apparently still very important; (ii) The data of the previous experiment were reproduced well with the tu-SPM. For the present kinematics, large deviations are observed from the tu-SPM and the ak-SPM lies closer to the data, albeit showing large discrepancies. The shape of several angular distributions is not reproduced by either SPM and one should conclude that neither of the two SPMs gives an accurate description of the data and both are thus lacking some higher-order (model-dependent) terms; and (iii) The cross-section prediction of the microscopic model is systematically above the data, both for the previous and the present data except for $\theta_\gamma \approx 100°$ and for the kinematics where there is a large asymmetry between the proton angles with $\theta_1 > \theta_2$ in which case the microscopic calculation comes very close to the data.

In conclusion, a proton–proton bremsstrahlung measurement of cross section and analyzing power has been performed at an incident energy of 190 MeV. Protons were detected using SALAD at forward angles, while plastic ball was employed to detect photons at backward angles. This experiment is a follow-up high-precision measurement in which the phase-space coverage of the first measurement [11] was extended in order to move towards the elastic channel by measuring lower energy photons. The results of two different types of calculations have been compared to the data, two soft-photon models (SPM) and a microscopic model. The relative energy of protons in the exit channel, E_{rel}, was introduced to have a measure of how far the kinematics is from the elastic limit. Neither the SPMs nor the microscopic calculation reproduce the data satisfactorily although values of A_y are in qualitative agreement. Contrary to the trend observed in the first measurement and our expectation from the soft-photon theorem, the agreement between the

cross-section data and calculations does not improve globally over the phase space when moving towards the elastic limit. This may have to do with the fact that the phase space covered in this measurement is still too far from the elastic limit to validate the predictions of the soft-photon theorem. Surprisingly, the cross-section data agree better with the predictions when $\theta_1 > \theta_2$. This behavior needs further investigation. In the multi-dimensional space of this reaction, we have not been able to find a single variable with which one can point to the source of these discrepancies. Extra handles to understand this simple, yet important reaction, can come from new measurements involving yet lower photon energies either using the same beam energy or reducing the beam energy. In this way, one is able to vary E_{rel} and $E_\gamma^{C.M.}$ independently. Such measurements require a different setup due to different ranges of particle energies. Given reasonable amount of beam time, more exclusive measurements such as spin-transfer or spin-correlation experiments are statistically not feasible. This can already be seen in the present analyzing power measurements from which it is not easy to draw any sensible conclusions regarding various theories.

Acknowledgements

References

[1] V.G.J. Stoks, R.A.M. Klomp, M.C.M. Rentmeester, J.J. de Swart, Phys. Rev. C 48 (1993) 792.
[2] R. Machleidt, F. Sammarruca, Y. Song, Phys. Rev. C 53 (1996) R1483.
[3] R.B. Wiringa, V.G.J. Stoks, R. Schiavilla, Phys. Rev. C 51 (1995) 38.
[4] J. Ashkin, R.E. Marshak, Phys. Rev. 76 (1949) 58.
[5] M.I. Sobel, A.H. Cromer, Phys. Rev. 132 (1963) 2698.
[6] D. Drechsel, L.C. Maximon, Ann. Phys. 49 (1968) 403.
[7] V. Herrmann, K. Nakayama, O. Scholten, H. Arellano, Nucl. Phys. A 582 (1995) 568.
[8] H. Huisman, et al., Phys. Rev. Lett. 83 (1999) 4017.
[9] H. Huisman, et al., Phys. Lett. B 476 (2000) 9.
[10] H. Huisman, et al., Phys. Rev. C 65 (2002) 031001R.
[11] M. Mahjour-Shafiei, et al., Phys. Rev. C 70 (2004) 024004.
[12] G.H. Martinus, et al., Phys. Rev. C 58 (1998) 686.
[13] G.H. Martinus, O. Scholten, J.A. Tjon, Few Body Systems 26 (1999) 197.
[14] M.D. Cozma, G.H. Martinus, O. Scholten, R.G.E. Timmermans, J.A. Tjon, Phys. Rev. C 65 (2002) 024001, nucl-th/0111039.
[15] M.D. Cozma, O. Scholten, R.G.E. Timmermans, J.A. Tjon, Phys. Rev. C 68 (2003) 044003.
[16] A.Yu. Korchin, et al., Nucl. Phys. A 602 (1996) 423.
[17] M.K. Liou, D. Lin, B.F. Gibson, Phys. Rev. C 47 (1993) 973;
M.K. Liou, R. Timmermans, B.F. Gibson, Phys. Rev. C 54 (1996) 1574.
[18] N. Kalantar-Nayestanaki, J. Mulder, J. Zijlstra, Nucl. Instrum. Methods Phys. Res. A 417 (1998) 215.
[19] N. Kalantar-Nayestanaki, et al., Nucl. Instrum. Methods Phys. Res. A 444 (2000) 591.
[20] A. Baden, et al., Nucl. Instrum. Methods 203 (1982) 189.
[21] M.C.M. Rentmeester, et al., Phys. Rev. Lett. 82 (1999) 4992.
[22] F.E. Low, Phys. Rev. 110 (1958) 974.
[23] E.M. Nyman, Nucl. Phys. A 160 (1971) 517.